# Relevant Material for Lecture 2

"Galaxies: Structure, Dynamics, and Evolution"

## 7.2 Mass distribution and dark matter in spiral galaxies

### Dark Matter Halos in Spiral Galaxies BT 10.1-6

measure rotation curve of cold gas
- H alpha (optical)
- CO (mm arrays)
- H I (vla, westerbork)

assume circular orbits:

$$\frac{v_c^2(r)}{r} = \frac{GM(<r)}{r^2}$$

The enclosed mass is directly given by

$$M(<r) = rv_c^2(r)/G$$

Isothermal sphere: $v_c = constant$, $\rho \propto r^{-2}$

Point Mass: $v_c \propto 1/\sqrt{r}$

Measurement in practice:

- Take edge-on system, measure maximum velocity of gas at each point
  possible problems: extinction, confusion

- Take inclined galaxies, measure velocities everywhere
  • Model by fitting a circular velocity field with unknown inclination and rotation curve



Historically, optical rotation curves like these on the following figure indicated for the first time the presence of dark matter.

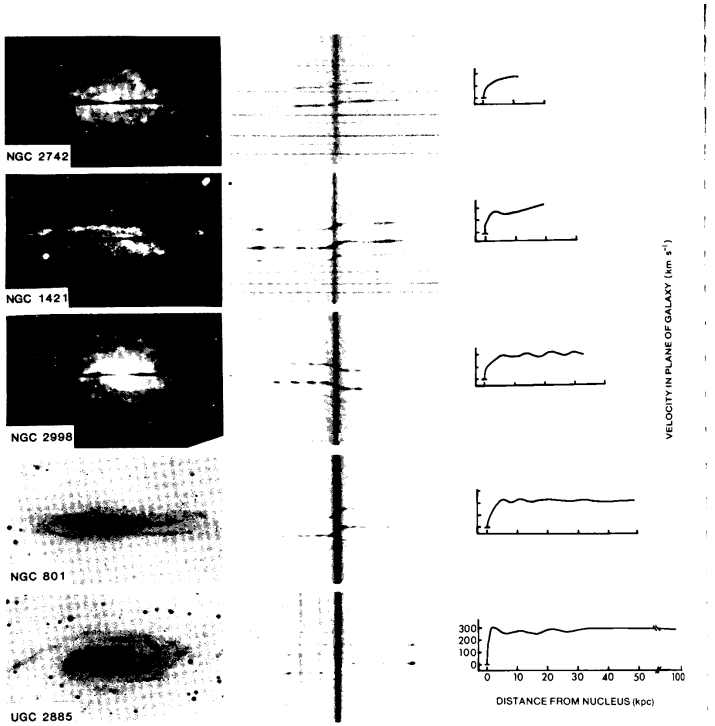


**Figure 10-1.** Photographs, spectra, and rotation curves for five Sc galaxies, arranged in order of increasing luminosity from top to bottom. The top three images are television pictures, in which the spectrograph slit appears as a dark line crossing the center of the galaxy. The vertical line in each spectrum is continuum emission from the nucleus. The distance scales are based on a Hubble constant $h = 0.5$. Reproduced from Rubin (1983), by permission of *Science*.

Very modern data are based on 21cm HI emission lines. The HI disks can often be followed to very large radii, and hence the rotation curve can be followed to well

model looks like:

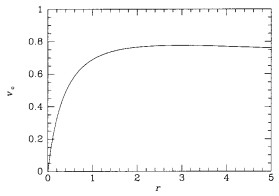


**Figure 8.31** A typical galactic circular-speed curve.

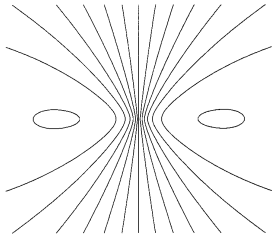

**Figure 8.32** The spider diagram generated by the circular-speed curve of Figure 8.31 when the system is viewed at inclination $i = 30°$ with the apparent major axis horizontal. The area contoured is a square 10 distance units on a side.

We can now model the galaxy. Take the surface brightness profile, and calculate the rotation curve if the mass-to-light ratio were constant:

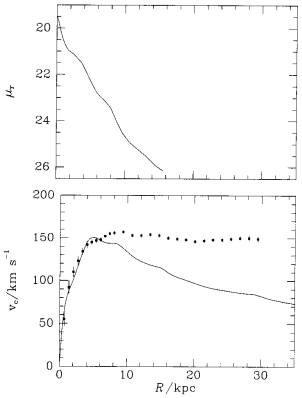


**Figure 8.35** The 21-cm circular-speed curve of the Sc galaxy NGC 3198 implies that most of the galaxy's mass lies beyond $R_{25}$. The upper panel shows the $r$-band surface brightness profile from Kent's CCD photometry. The curve in the lower panel shows the circular-speed curve derived from this and the observed HI mass under the assumption that $\Upsilon_r = 3.8\Upsilon_r(\odot)$. The dots in the lower panel show the circular-speed curve derived from the 21-cm velocity field. [After Begeman (1987) using data kindly provided by K. Begeman]



Obviously, an additional mass component is necessary to explain the rotation curve.

Fit rotation curves:

Constant M/L for starlight
add halo, with $\rho = \rho_0/(1 + (r/a)^2)$

Example for NGC 3198

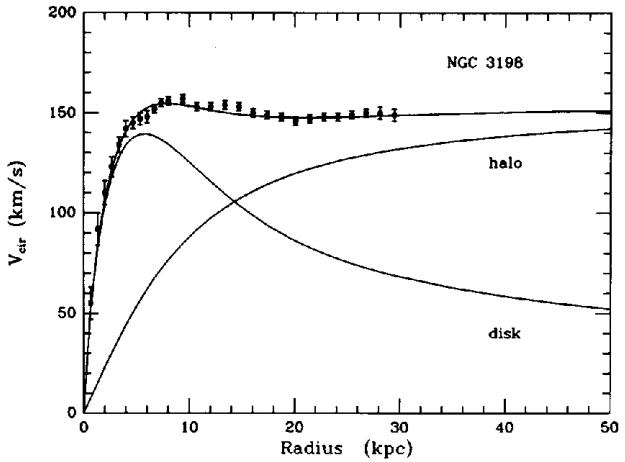


**Figure 10-2.** The Sc galaxy NGC 3198. Top: neutral hydrogen column density contours superimposed on an optical photograph. Bottom: circular-speed curve plus model fits using an exponential disk with constant mass-to-light ratio and the halo density profile (10-10). The model curve is for the maximum possible disk mass-to-light ratio. The horizontal scale assumes $h = 0.75$. Reprinted from van Albada et al. (1985), by permission of *The Astrophysical Journal*.

Problems: The fit is never unique. Different M/L's for the disk, and different values of $a, \rho_0$ for the

halo will give fits which are all good.
Hence: it is very hard to determine how much of the mass is due to the halo, within the outer most radius

Solution: determine the "minimum halo mass", by calculating "maximum disk". But this is only the minimum !

Various authors have assembled large samples of galaxies with rotation curves. An example: Casertano and van Gorkom (1991, AJ 101, 1231)

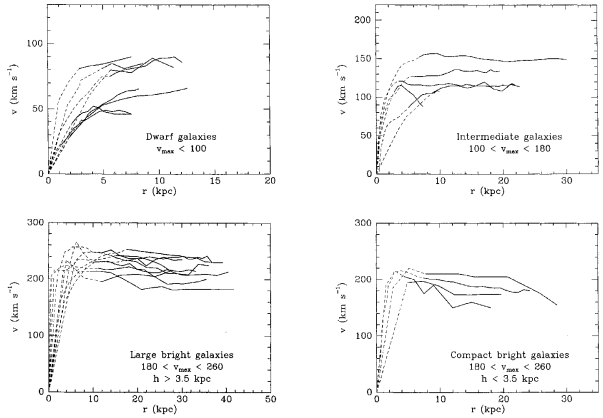


FIG. 5.Comparison of the 28 extended rotation curves shown in Fig. 4. Each panel refers to one of the four galaxy groups described in the text: dwarf, intermediate, bright and bright compact galaxies. The rotation curves are drawn with thick solid lines beyond an inner fiducial radius corresponding to two-thirds of the optical radius. A systematic change in shape is apparent: rotation curves of dwarf galaxies rise, often out to the last measured point; those of intermediate galaxies are generally flat, with some exceptions (rising for NGC 247 and declining for NGC 7793); those of bright galaxies fall, weakly for large ones, more steeply for compact galaxies.

Resulting rotation curves:

- Rapid rise near center
- nearly flat out to most distant point, with some variations:
  dwarf galaxies: still rising
  intermediate galaxies: flat



large bright galaxies - slightly falling, compact galaxies, falling slightly more

- Never Keplerian - always a lot of dark matter !

**Homework Assignment:**
1) Calculate the total mass, the mass in the disk, and the mass in the halo for NGC 3198 at a radius of 30kpc. Use the decomposition into components shown in the figure above.

## 7.5 Clusters of galaxies BT 10.2-4

measure redshifts of cluster galaxies

velocity dispersions of 1000 km/s or higher are measured !

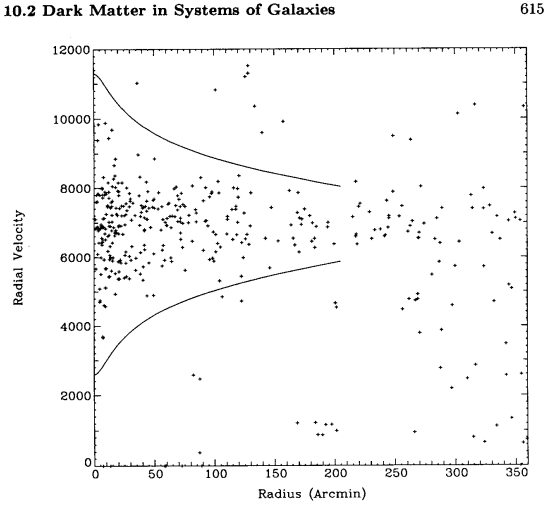


**Figure 10-4.** Line-of-sight velocities of galaxies in the Coma cluster (in $\mathrm{km\,s^{-1}}$) as a function of distance from the cluster center in minutes of arc (Kent & Gunn 1982). The curves mark the authors' estimate of the boundary between cluster members and interlopers. At the distance of Coma 1 arcmin = $20h^{-1}$ kpc. Reprinted by permission from *The Astronomical Journal*.

Kent and Gunn 1982



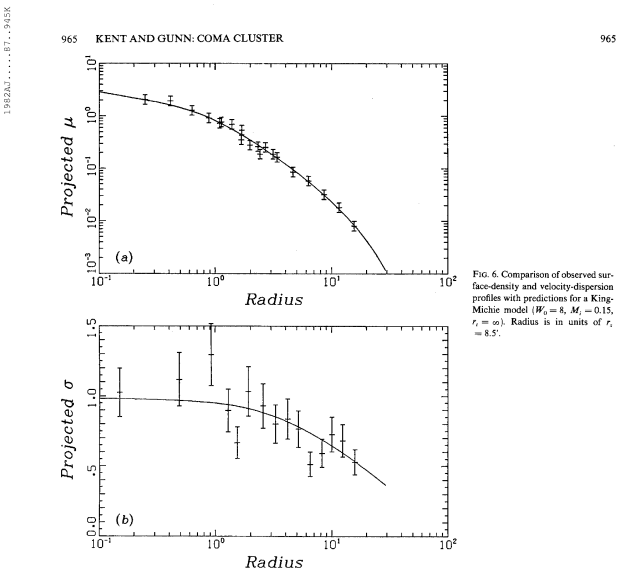


FIG. 6. Comparison of observed surface-density and velocity-dispersion profiles with predictions for a King-Michie model ($W_0 = 8$, $M_j = 0.15$, $r_t = \infty$). Radius is in units of $r_c = 8.5'$.

Careful model shows: total mass is $2 \times 10^{15} M_\odot$ (H0 = 70 km/sec/Mpc).

Total amount of light: 279 galaxies brighter than $L_*$, $L_* = 0.7\ 10^{10} L_\odot$. Total amount of light is $4.33 \times L_* \times N = 0.8\ 10^{13} L_\odot$

Hence mass to light ratio = $M/L = 210^{15}/0.810^{13} = 250\ M_\odot/L_\odot$.

Similar study (Kent and Sargent) Perseus: $M/L_V = 420\ M/L_\odot$

Typical masses of clusters: $10^{14} - 10^{15}\ M_\odot$

Normal galaxy: $M_{LV} < 10 M/L_\odot$, hence a lot of dark matter.

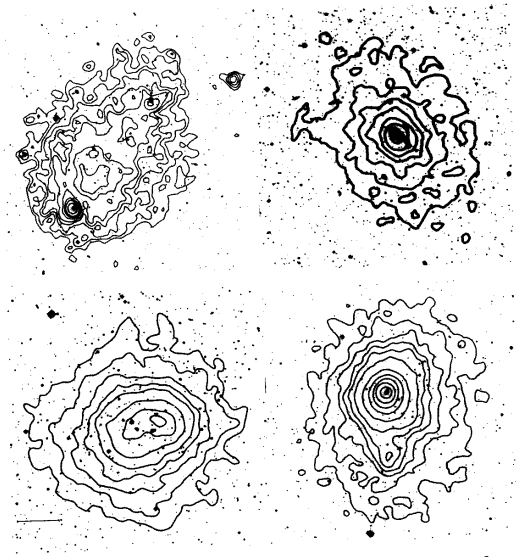

**Figure 10-5.** X-ray surface-brightness contours superimposed on photographs of several clusters of galaxies. Clockwise from top left, the clusters are A1367, A262, A85, and A2256 (see Jones & Forman 1984).

Similar mass determinations from gas . Temperatures can now be measured easily with X-ray satellites. Results:

- Confirms high masses

Mass budget:
- Gas mass fraction 20-30 % of total mass
- Star mass fraction $< 10$ % of mass
- Remaining: dark matter 60-70 % !



## 7.6 Dark matter in universe as a whole BT 10.3-1

The emissivity of light in the universe in the V band is

$$j_0 = 1.7 \pm 0.610^8 h L_\odot Mpc^{-3}$$

The critical density for the universe is:

$$\rho_c = \frac{3H_0^2}{8\pi G}$$

This density is enough to stop the expansion at $t =$ infinity

Define the density parameter $\Omega_0 = \rho_0/\rho_c$, where $\rho_0$ is the actual density of the universe

Express $\Omega_0$ in terms of $M/L$ ratio of galaxies:

$$\Omega_0 = 6.110^{-4} h^{-1} M/L/(M/L)_\odot$$

The critical mass-to-light ratio for $\Omega = 1$ is given by

$$M/L_c = 1600h(M/L)_\odot$$

Clusters imply $M/L_c = 300 - 600h(M/L)_\odot$, hence more realistic values are

$$\Omega_0 = 0.2 - 0.4$$

from clusters.

## other indicators give:

**Table 10-2.** Estimates of the density parameter

| Method | $\Upsilon_V/\Upsilon_\odot$ | $\Omega_0$ |
|---|---|---|
| Solar neighborhood | 5 | $0.003h^{-1}$ |
| Elliptical galaxy cores | $12h$ | 0.007 |
| Local escape speed | 30 | $0.018h^{-1}$ |
| Satellite galaxies | 30 | $0.018h^{-1}$ |
| Magellanic Stream | $> 80$ | $> 0.05h^{-1}$ |
| Rotation curve of NGC 3198 | $> 28h$ | $> 0.017$ |
| X-ray halo of M87 | $> 750$ | $> 0.46h^{-1}$ |
| Local Group timing | 100 | $0.06h^{-1}$ |
| Groups of galaxies | $260h$ | 0.16 |
| Clusters of galaxies | $400h$ | 0.25 |
| Virgocentric flow | – | 0.25 |
| Nucleosynthesis | – | $(0.01 - 0.05)h^{-2}$ |
| Inflation | – | 1 |

NOTES: All lines except the last three are based on the luminosity density (10-24). Nucleosynthesis estimate omits density in non-baryonic matter. Several methods, such as Local Group timing and X-ray halo of M87, depend on $h$ in complicated ways, and this dependence has been suppressed. See text for further detail.



Measurements on the largest scales concern those caused by inflows around clusters (BT 10.3-2)

matter falls into clusters of galaxies. Assume that the density contrast of the cluster is the same as that of the light

$$\frac{\rho_{cluster}}{\rho_{universe}} = \frac{j_{cluster}}{j_{universe}} = \delta$$

where $j$ is emissivity. The total mass of the cluster is proportional to $\Omega_0$

$$Mass \propto R^3\rho \propto \delta\rho_{universe} \propto \delta\Omega_0$$

Hence, the acceleration of galaxies outside the cluster will depend on $\Omega_0$.

Example: determine $\Omega_0$ from "Virgo centric infall"

## Scaling relations

If galaxies all form at some fixed redshift, we might expect that they all have the same mean density. This would apply to their halos, obviously:

$$< \rho_{halo} >= constant$$

The implication is that mass is simply related to halo size:

$$M \propto < \rho > R^3$$

where $R$ is the halo size.
We assume that the halo is isothermal with a density profile

$$\rho = \rho_0 r^{-2}$$

Hence the circular velocity $v_c$ is constant with radius.
The total mass is given by

$$v_c^2/R = GM/R^2$$

$$M = Rv_c^2/G$$

Now use $R \propto M^{1/3}$, hence

$$M \propto M^{1/3} v_c^2$$

take $M$ to the left side of the equation

$$M^{2/3} \propto v_c^2$$

or

$$M \propto v_c^3$$

This relation is very close to that observed for galaxies

- Tully-Fisher for spirals: $L \propto v_c^{(3-4)}$
- Faber-Jackson for ellipticals: $L \propto \sigma^{(3-4)}$

both relations have significant scatter - cannot be compared to the narrow main sequence for stars

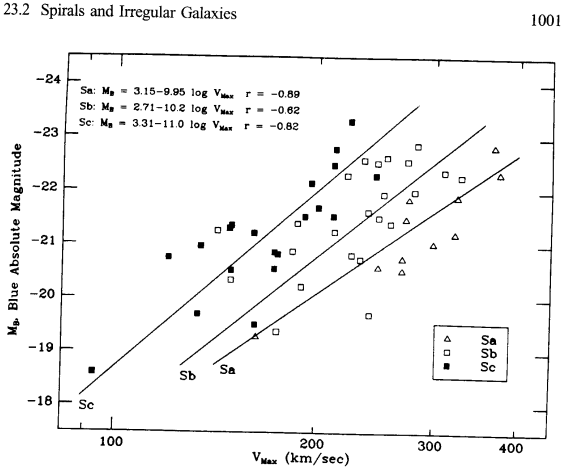


**Figure 23.9** The Tully–Fisher relation for early spiral galaxies. (Figure from Rubin et al., *Ap. J.*, *289*, 81, 1985.)



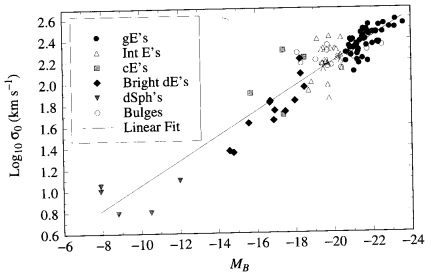


**Figure 23.31** The Faber–Jackson relation represents a correlation between central velocity dispersion and luminosity. The relation is a consequence of the virial theorem. (Data from Bender et al., *Ap. J.*, *399*, 462, 1992.)

The fact that galaxies follow these relations is remarkable, because it not at all necessary for galaxies to have such a relation from "simple" dynamics.

The relations are even more remarkable since the prediction is for the mass, not the light, of galaxies to follow such a relation. As a consequence, there is a likely, simple relation between mass and light

$$M_{halo} \propto L_{stars}???$$

The explanation for this relation is usually the following: Each dark matter halo has some fraction $f$ of its mass in baryons (hydrogen mainly). These baryons sink to the center, and form stars. The light of the stars is proportional to the mass in baryons, which is proportional to the mass in dark matter. This simple explanation might just work...

### 3.2 Internal structure of disks

Our own galaxy gives a unique insight into disks: we can look at individual stars !

From good spectra and photometry, one can derive velocities, stellar age, and metal abundance.

Basic results:

- the velocity dispersion of a population of stars depends on the age. The older the population of stars, the higher the velocity dispersion.

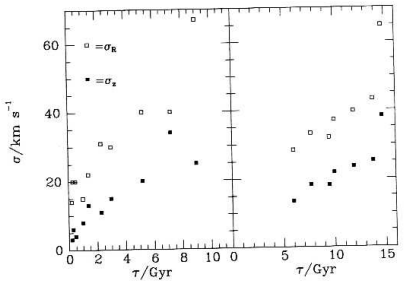


**Figure 10.20** Velocity dispersion versus age as determined by Jahreiss & Wielen (1983) (left panel) and by the Danish group (right panel). Aside from a difference in the age scales used in these studies, the two determinations are broadly consistent with one another. [From data published in Jahreiss & Wielen (1983) and in Strömgren (1987)]

Interestingly, the velocity dispersions in the 3 directions change in very characteristic ways - with, for example, $\sigma_\phi/\sigma_r$ being quite constant.

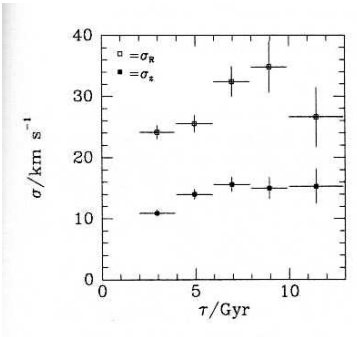


**Figure 10.22** The variation with age $\tau$ of the radial and vertical velocity dispersions of 556 stars with $-0.15 < [\mathrm{Fe/H}] < 0.15$. For this sample $\sigma_\phi/\sigma_R = 0.61 \pm 0.02$ with no statistically significant dependence of the ratio upon $\tau$. [From data published in Strömgren (1987)]

How can this 'disk heating' trend be explained ?
several mechanisms have been proposed
heating due to interactions with spiral arms
heating due to interactions with molecular clouds
heating as a left-over from formation
heating due to infall of satellites
These all predict different trends - and none fit the data very well.

- relation between age and metallicity

Stars in the disk have a wide range in metallicity. The figure below shows the result

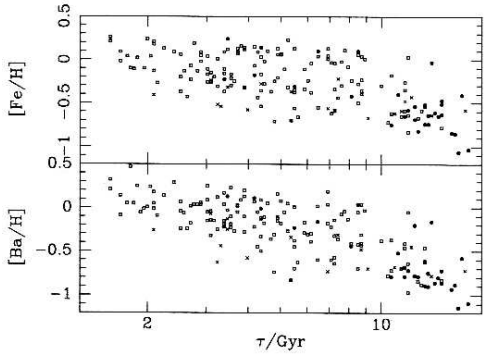


**Figure 10.18** The dependence upon age of the abundances of iron and barium. The characteristic Galactocentric radius of each star, $R_m$, is indicated by different symbols: • ⇒ $R_m < 7$ kpc; □ ⇒ $7\,\text{kpc} < R_m < 9\,\text{kpc}$; × ⇒ $R_m > 9$ kpc. [After Edvardsson *et al.* (1993) from data kindly supplied by B. Edvardsson]

Old stars have a lower metallicity than young stars. This suggests that the metallicity of the gas (from which the stars formed) increased gradually with time. This is expected to happen, due to metals being injected into the gas by stellar winds and supernovae.

However, notice the large scatter ! The inter stellar medium did not have a simple metallicity-age relation !

- The abundance ratios of elements also vary as a function of metallicity

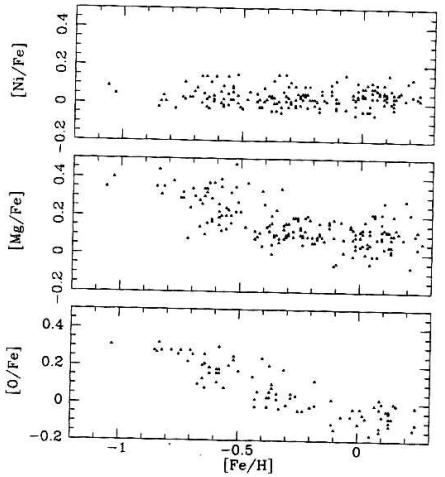


**Figure 10.17** The dependence upon the abundance of Fe of the ratios of Ni, O and Mg to Fe. The ratio of Ni to Fe is flat because these elements are produced alongside one another. The ratios of O and Mg to Fe decline with increasing Fe abundance because O and Mg, which are produced by short-lived stars, were formed before the disk became heavily polluted by iron from type Ia supernovae, which have long-lived progenitors. [After Edvardsson *et al.* (1993) from data kindly supplied by B. Edvardsson]

This can be due to the fact that different enrichment mechanisms produce metals in different ratios. For example, supernovae type Ia have different ratios from type II supernovae. We'll return to this later. Type Ia supernovae play an important role for iron, but they probably occur well after type II's . Hence, the ratios will change with time.

- The thick disk

The disk is not "simple" When studied in detail, it has an "extension" which is often called the thick disk. The thin disk is the part which dominates at small distances from the plane. The density of the thick disk becomes comparable to that of the thin disk around 1.5 kpc above the plane, and dominates

above that. Both the thin and the thick disk separately go like $\rho \propto \exp -(z/z_h)$, where $z_h$ is the scale height.

This is illustrated in the figure below

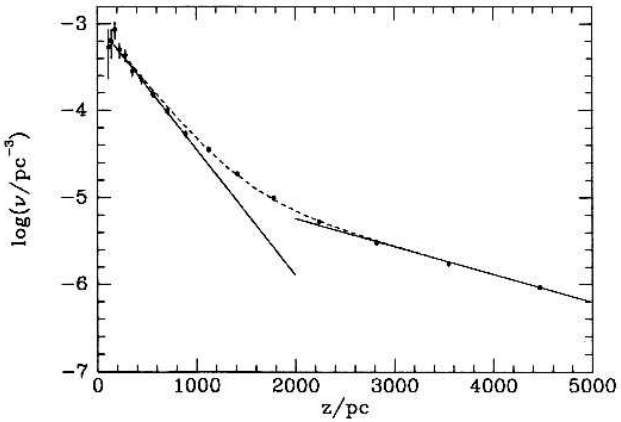


**Figure 10.25** The space density as a function of distance $z$ from the plane of MS stars with absolute magnitudes $4 \leq M_V \leq 5$. The full lines are exponentials with scale heights $z_0 = 300\,\mathrm{pc}$ (at left) and $z_0 = 1350\,\mathrm{pc}$ (at right). The dashed curve shows the sum of these two exponentials. [From data published in Gilmore & Reid (1983)]

The thick disk is also apparent when the relation between age and metallicity is plotted.

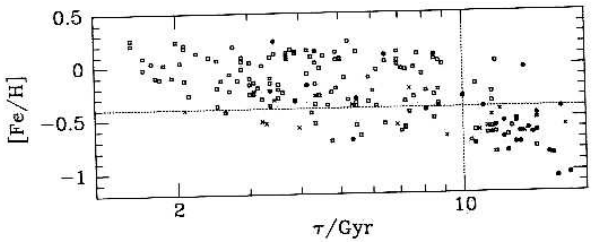


**Figure 10.26** A potential division of stars between the thin and thick disks. Stars above and to the left of the dotted lines are assigned to the thin disk, while those below and to the right of the lines are assigned to the thick disk.

Thick disk stars are more metal poor and older. Caused by a merger ? Or "initial conditions ? "

### 3.3 Other components in spiral galaxies

#### 3.3.1 Gas

Obviously, spiral galaxies have gas (neutral hydrogen, molecular hydrogen, and ionized hydrogen). Most of the gas resides in the disk. Some gas disks are warped in the outer parts - as if somebody is toying with the galaxy. Typical gas masses are around $3 - 6e9\ M_{\odot}$. In galaxies like our own galaxy, the amount of gas in molecular and neutral form is comparable. Molecular gas tends to be more centrally concentrated.

An example of a strongly warped galaxy: NGC 4013. The warp starts at the edge of the optical disk

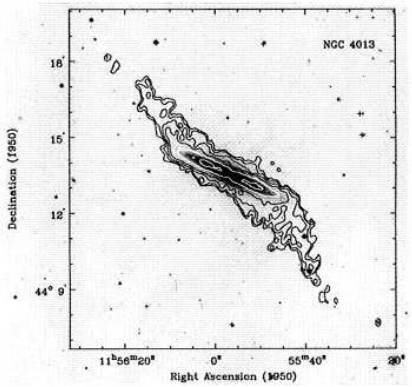


**Fig. 1.** Total H I map of NGC 4013 superposed on the optical image. Contours are at levels of 1.02 $10^{20}$, 2.03 $10^{20}$, 4.06 $10^{20}$, 8.13 $10^{20}$, 20.32 $10^{20}$, and 46.82 $10^{20}$ H-atoms cm$^{-2}$. The resolution is indicated by the beam in the lower right corner

Molecular and Neutral gas in NGC 6946. The neutral gas is traced best by CO emission. Here the CO emission is shown, super imposed on the SDSS image of the galaxy. The CO is strongly peaked at the center.

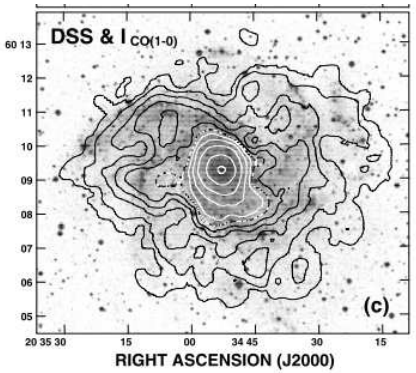


FIG. 2.—CO(1–0) integrated and peak intensity maps for NGC 6946. (*a*) CO(1–0) integrated intensity map. The gray scale ranges from 0 to 50 K km s$^{-1}$. The contour levels are 1, 2.5, 5, 7.5, 10, 12.5, 15, 20, 30, 50, and 70 K km s$^{-1}$. The 55″ (FWHM) circular beam is displayed at the lower left. (*b*) CO(1–0) peak intensity map. The gray scale ranges from 0 to 0.52 K. The contour levels are 0.10, 0.17, 0.23, 0.30, 0.37, and 0.43 K. (*c*) DSS uncalibrated optical image with the same $I_{10}$ contours shown in (*a*).

Here is the H I 21-cm emission line map:

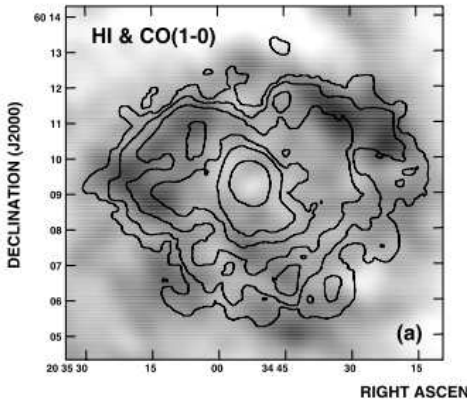


FIG. 7.—CO and H I in NGC 6946. (*a*) $I_{H\,I}$ (*gray scale*) and $I_{10}$ (*contours*). The gray scal and 35 K km s$^{-1}$. (*b*) $I_{H\,I}$ (*gray scale*) and $I_{21}$ (*contours*). The gray scale ranges from 0 to

And here is shown the gas surface density in molecular

and neutral form (assuming some conversion of CO emission to $H_2$ surface density).

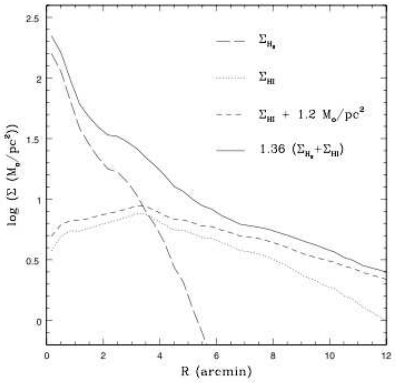


FIG. 8.—Gas surface density vs. radius in NGC 6946. Plotted are $\Sigma_{H_2}$ derived using the standard conversion factor; $\Sigma_{H_2}$ from the observed emission; $\Sigma_{H_2}$ increased for the VLA missing flux estimate; and the total gas surface density increased by a factor of 1.36 to include the He and heavier element content. All have been corrected for inclination ($\cos i$). At our assumed distance of 6 Mpc, $1' = 1.75$ kpc.

The $H_2$ dominates at the center, the H I at the outer parts. Why ? $H_2$ can only form if the gas is shielded from UV radiation. Hence at high surface brightness, and at high metallicity, more dust will be present, and more shielding is possible.

### 3.3.2 Halo

Our galaxy also has stars which move very differently from the disk stars. See, for example, the figure below

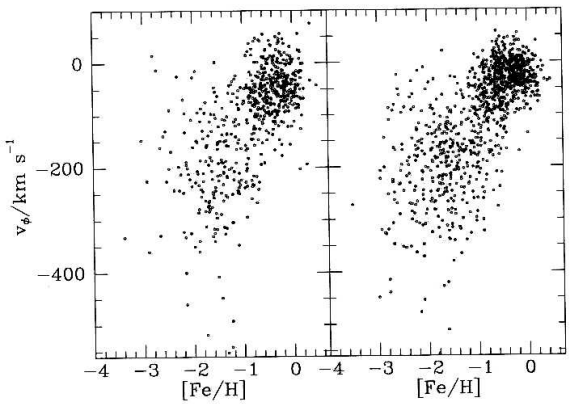


**Figure 10.36** [Fe/H] versus $v_\phi$ from Nissen & Schuster (1989) (left panel, 611 stars) and Carney *et al.* (1996) (right panel 1022 stars). [From data kindly supplied by B. Carney and P. Nissen]

The stars have much lower metallicity, and the system of stars hardly rotates around the center. These are halo stars. They were probably formed much earlier than the disk stars - although many astronomers think they may have been deposited in the halo by mergers !

Globular clusters also form part of the halo, and are easy to track !

One might expect the halo to be regular - but recent evidence shows that this might not be the case.

The image below shows the distribution of stars on the sky in the halo - as derived from the SDSS catalogue. Stars are selected in a narrow color interval and magnitude interval. They lie at roughly the same distance. The distribution appears not to be smooth

**Fig. 3**
Stellar halo of the Milky Way as seen by SDSS. The gray scale denotes the logarithm of the number density of $0.2 \leq g - r \leq 0.4$ stars per square degree in eight different magnitude (therefore mean distance) slices; a Lambert azimuthal equal-area polar projection is used. The black areas are not covered by the SDSS DR5, and reflect the great circle scanning adopted by the SDSS when collecting its imaging data. Apparent "hot pixels" are stellar overdensities from globular clusters and dwarf galaxies.

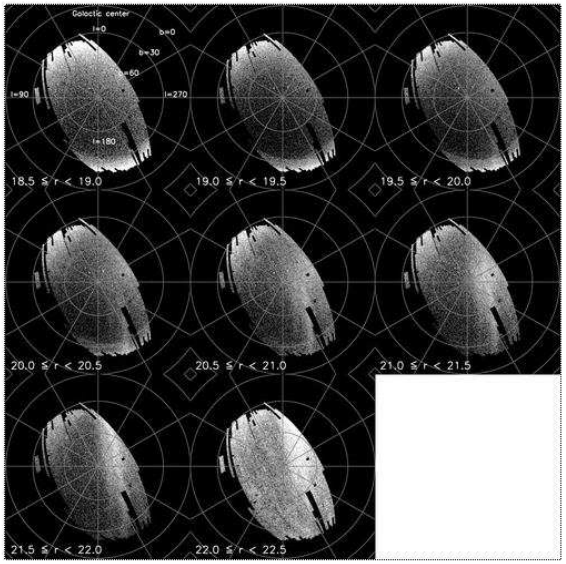


When we subtract a smooth model for the halo, we observe the following residuals in the density distribution

**Fig. 10**
Residuals of the mean stellar density ($\mathrm{data} - \mathrm{model}$) from the best oblate model $(\alpha_{\rm in}, \alpha_{\rm out}, r_{\rm break}, c/a) = (-2.2,\ -3.5, 20\ \mathrm{kpc},\ 0.7)$. The panels show eight different distance slices, and have been smoothed using a $\sigma = 42'$ Gaussian. The gray scale saturates at ±60% deviation from the model density, and white represents an observed excess over the smooth model prediction.

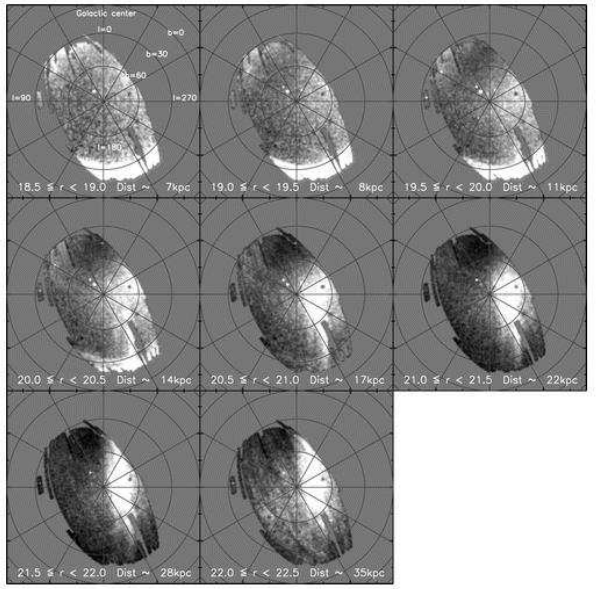


These kind of residuals can be reproduced in merger formation models for the halo. Some examples are shown below. The simulations have been "observed" in the same way as the original stars in our halo

**Fig. 13**
Residuals (SDSS or simulations minus the smooth model) smoothed using a $\sigma = 42'$ Gaussian from the best oblate model fits for the SDSS data (*top left panel*) and for the 11 simulations from Bullock & Johnston (2005). We show only the $20 \leq r < 20.5$ slice, corresponding to heliocentric distances ~14 kpc. The gray scale saturates at ±60% from the smooth model density.